

# KINEMATIC FEATURES OF REACH AND GRASP MOVEMENTS IN STROKE REHABILITATION USING ACCELEROMETERS

Julien Stamatakis<sup>1</sup>, Adriana Gonzalez<sup>1</sup>, Benoit Caby<sup>1</sup>, Stephanie Lefebvre<sup>2,3</sup>,  
Yves Vandermeeren<sup>2,3</sup> and Benoit Macq<sup>1</sup>

<sup>1</sup>*Institute of Information and Communication Technologies, Electronics and Applied Mathematics  
Université catholique de Louvain, Louvain-la-Neuve, Belgium*

<sup>2</sup>*Institute of NeuroSciences, Université catholique de Louvain, Brussels, Belgium*

<sup>3</sup>*Department of Neurology, Cliniques Universitaires de Mont-Godinne, Université catholique de Louvain, Yvoir, Belgium*

Keywords: Accelerometers, Codamotion, Kalman Filter, Kinematic Analysis, Stroke.

Abstract: Rehabilitation is an essential process to recover impaired motor functions after stroke. Typically, visual marker-based systems such as the Codamotion are used, as kinematic analyses seem to be an excellent tool to quantify objectively the effects of rehabilitation processes. However, this solution remains expensive. A low-cost accelerometer-based system has been developed and its performances were compared to those of the Codamotion system, used as a gold standard. Thanks to a model for prediction and an error model Kalman filter, the recorded signals were broken up into gravity and dynamic accelerations components that were placed in a global frame and compared to the Codamotion signals. The vertical z-axis was well reconstructed and used as a basis for kinematic analyses. Different features expressing movement speed, control strategy or movement smoothness have been computed from both systems and compared. Despite the fact that some of them showed differences between both systems, the accelerometer-based system computed features with a discriminant power comparable to the ones derived from the Codamotion. In conclusion, this accelerometer-based system is a low-cost alternative to expensive visual marker-based systems that could be extensively used for rehabilitation processes in routine clinical practice or even at home.

## 1 INTRODUCTION

Stroke is one of the leading causes of brain function impairment, affecting motor, visual and speech abilities. The inability to perform motor tasks has major consequences on daily-life activities, leading to disability and loss of autonomy. Although some of those motor functions may be recovered spontaneously, a rehabilitation therapy is needed in most cases (Zhou et al., 2008). It has been shown that targeted rehabilitative strategies can help the patient to regain and relearn the impaired motor skills (Zhou et al., 2008; Cirstea and Levin, 2007; Caimmi et al., 2008). To develop and refine such strategies, the patient motions need to be monitored, in order to follow the evolution of the treatment, to supervise the correct performances of the rehabilitation and to help correcting some movements (Zhou and Hu, 2008). Rehabilitation has to focus on daily-life tasks such as reaching and grasping an object. This relatively complex task involves the selection and control of the finger

grip aperture according to the size and shape of an object, as well as the transport of the hand towards the target. Several studies have been dedicated to the evaluation of revalidation methods and treatments (Caimmi et al., 2008; Wu et al., 2000). Kinematic analyses seem to be an excellent and very sensitive tool to quantify the effects of rehabilitation processes on motor performances (Caimmi et al., 2008). Features representing speed, accuracy or efficiency can be extracted all along the rehabilitation process (Lang et al., 2006) in order to assess the evolution of the recovery. Several systems have been developed over the past decade in order to track human motion for kinematic analyses (Zhou and Hu, 2008). Visual marker-based tracking systems such as VICON or Codamotion are often used as gold standards because of their accuracy. However, these systems are expensive and cannot currently be applied at home or in the daily-life environment of the patients. Other systems based on inertial sensors like accelerometers and gyroscopes (Kavanagh and Menz, 2008) have also been devel-

oped. They are small, low-cost and well adapted for portable devices. These systems are widely used in the medical field to detect physical activity, to prevent falls of the elderly or to track upper limb motions (Zhou et al., 2008). Multiple inertial sensors can be combined but the size is then increased and the calibration method becomes more complex.

In this paper, the development of a low-cost inertial system based exclusively on accelerometers for kinematic analyses is proposed. Such a system is physically compact and can be used in daily-life environments. Few studies have focused on the exclusive use of accelerometers. Indeed, since the measurement contains gravitational, kinematic and noise components, the dynamic acceleration is difficult to extract without some extra information. The extraction of the dynamic acceleration in each sensor frame is based on the frequential properties of the movements, as proposed in Luinge and Veltink (2004). These accelerations are then placed in a global frame through a frame transformation. This system is used to extract kinematic features from reach and grasp movements that are compared to those extracted from the Codamotion system, used as ground truth.

## 2 MATERIAL AND METHODS

The Codamotion system (Charnwood Dynamics, Rothley, UK) is based on active markers and infrared cameras, allowing the 3-D measurement of each marker position. In the global Codamotion frame, the horizontal  $x$  axis is parallel to the movement direction, the horizontal  $y$  axis is perpendicular to  $x$  and  $z$  is the vertical axis. At a 3 m distance, the accuracy is  $\pm 1.5$  mm in  $x$  and  $z$  axes, and  $\pm 2.5$  mm in  $y$  axis for peak-to-peak deviations from actual position (Zhou and Hu, 2008). The sampling frequency is set to 200 Hz. The low-cost accelerometer system is composed of three 3-axis accelerometers, recording  $\pm 2.5$  g accelerations at the sampling rate of 66.67 Hz ( $1g = 9.81m/s^2$ ). In each sensor frame, the  $x$  axis is tangent to the limb,  $y$  is horizontally perpendicular to  $x$  and  $z$  is the normal axis to the limb. The accuracy on the accelerations is  $\pm 0.01$  g. Accelerometers have been calibrated using a minimization function based on the norm and direction of the gravity field. All data have been processed with Matlab (MathWorks, Natick, MA, USA). Subjects were recruited at Cliniques Universitaires UCL de Mont-Godinne; they provided written informed consent. This research protocol has been approved by the local ethical committee. Two hemiparetic stroke patients ( $mRS = 2$ ) and three healthy volunteers have

been included. Each subject had to execute 15 reach and grasp movements at comfortable speed. They were seated on a chair in front of the target, which was placed at a comfortable reaching distance, i.e. 90% of the total arm length. Each movement began with the hand resting on the legs. Sensors and active markers were placed on the index nail, thumb nail and on the wrist of the most affected arm for the patients and on the dominant hand for the healthy volunteers, as illustrated in Figure 1. The results are presented for the sensor and the marker that were placed on the wrist.

In order to extract kinematic features of the reach and grasp movements, the dynamic accelerations due to movements were extracted from the accelerometer signals using a Complementary Kalman Filter. The dynamic accelerations were expressed in the Codamotion global frame, instead of the sensor frame, to compare the reconstructed signal to the Codamotion signal in each axis. Then, some of the most commonly used features were computed for both systems and compared. The first feature is the Total Movement Time (TMT) (Trombly, 1993; Chang et al., 2005; Caimmi et al., 2008), computed as the time necessary to operate the whole reach and grasp movement; it is supposed longer for hemiparetic patients (Lang et al., 2006; Michaelsen et al., 2004). The second one is the number of Movement Units (MU), which allows to evaluate the smoothness of the movement (Trombly, 1993; Wu et al., 2007). A MU represents an increase of more than 10% of the maximum velocity between adjacent minimum and maximum in the velocity profile; it is supposed higher for pathological patients (Chang et al., 2005) since they have numerous, corrective and small movements. The third feature is the Normalized Jerk (NJ), defined in (1), where  $T$  is the total movement time,  $j$  is the jerk, i.e. the derivative of the acceleration, and  $D$  is the total distance of the reach and grasp movement path in space. This represents another feature to evaluate the smoothness of the movement, that is supposed to be lower for healthy subjects (Caimmi et al., 2008; Chang et al., 2005).

$$NJ = \sqrt{\frac{T^5}{2D^2} \int_{T_{start}}^{T_{stop}} j^2(t) dt} \quad (1)$$

The other features are the Peak Wrist Velocity (PWV) and the percentage time to reach this value (TPWV) (Trombly, 1993; Michaelsen et al., 2004; Lang et al., 2006; Chang et al., 2005). PWV is usually used to reflect the level of force generation (i.e. a high PWV is indicative of a high level of force generation) while TPWV reflects the control strategy (Chang et al., 2005) (i.e. TPWV will express whether the peak velocity is generated early or late in the move-

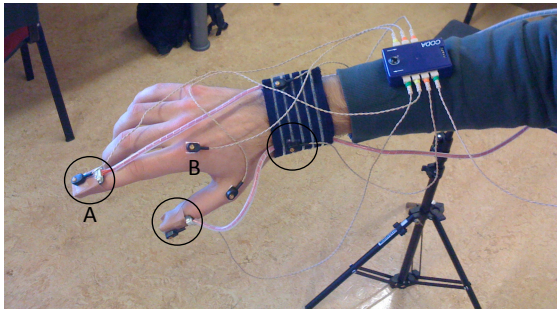


Figure 1: A. The accelerometers are placed on the finger nail, thumb nail and on the wrist. B. The active markers are placed above the accelerometers; the other markers are not used here.

ment). Both are supposed to be lower for the hemiparetic patients.

### 3 COMPLEMENTARY KALMAN FILTER

Although accelerometers do not depend on any external reference, they are bound to the gravity field and therefore their output signal is dependent of both the tilt angle and the actual acceleration. The first step in order to recover the accelerations due to movements ( $\mathbf{a}$ ) is thus to remove the gravity ( $\mathbf{g}$ ) components from the recorded signals ( $\mathbf{y}$ ). The signal is also affected by the bias ( $\mathbf{b}$ ), an intrinsic parameter of the accelerometer, that is reflected by an offset in the output signal.

$$\mathbf{a} = \mathbf{y} - \mathbf{g} - \mathbf{b} \quad (2)$$

Luinge and Veltink (2004) have worked on the extraction of the gravity and offset components from the accelerometer signal, considering as noise the acceleration component caused by movement. They stated that when the movement acceleration is sufficiently small in comparison to the gravity, the accelerometer can be used as an inclinometer. To perform such an extraction, they used a Complementary Kalman Filter. In this paper, the design is based on their method but instead of extracting the gravity and the offset, the idea is to extract the dynamic acceleration and the gravity.

The Complementary Kalman Filter or error-state Kalman Filter enables to combine two media (Higgins, 1975). It takes one as reference, works with the estimation of the difference between them and uses this estimation to update the other one (Welch and Bishop, 2001). It is often used to combine two sensors but, in this case, it combines one sensor and one prediction step as described in Figure 2. Furthermore, it allows the use of a linear Kalman filter while

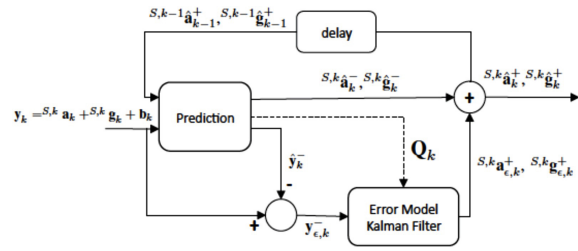


Figure 2: Complementary Kalman Filter with sensor and prediction values as inputs. The superscript  $-$  represents an *a priori* value and the superscript  $+$  represents an *a posteriori* value. A hat on the top of a symbol is used to indicate an estimation.  $k$  represents the current value and  $k - 1$  the one of the previous time step. The superscript  $S$  means that values are expressed in the Sensor frame while the superscript  $G$  means that values are expressed in the Global frame (Codamotion).

non-linear processes can be used during the prediction step. Here, an autoregressive (AR) model is set up.

The *a posteriori* estimates of the acceleration and gravity ( $S,k-1 \hat{\mathbf{a}}_{k-1}^+, S,k-1 \hat{\mathbf{g}}_{k-1}^+$ ) from the previous time step are used to make an *a priori* estimation of the acceleration and gravity, and thus to predict the sensor output vector  $\hat{\mathbf{y}}_k^-$ . The difference  $\mathbf{y}_{e,k}^-$  between the *a priori* predicted accelerometer output  $\hat{\mathbf{y}}_k^-$  and the actual output  $\mathbf{y}_k$  represents the *a priori* prediction error of the acceleration and gravity ( $S,k \mathbf{a}_{e,k}^-, S,k \mathbf{g}_{e,k}^-$ ). Then, the Kalman filter uses  $\mathbf{y}_{e,k}^-$  and the variance of the predicted components  $\mathbf{Q}_k$  to generate the *a posteriori* prediction error ( $S,k \mathbf{a}_{e,k}^+, S,k \mathbf{g}_{e,k}^+$ ) that will be used for the update of the acceleration and gravity predictions, resulting in their *a posteriori* estimations ( $S,k \hat{\mathbf{a}}_k^+, S,k \hat{\mathbf{g}}_k^+$ ).

This model is only valid if the accelerometer output signal meets the conditions exposed by Luinge and Veltink (2004). As shown in Figure 2, the Complementary Kalman Filter is composed by two phases : one for the prediction and the other for the error model Kalman filter. The prediction phase consists in modeling the behaviour of acceleration and gravity signals for specific movement, as presented for gravity in Luinge and Veltink (2004). The acceleration is modeled as an AR process, which is a time series analysis model based on the previous weighted outputs of the system (3). The AR modeling process is based on the spectrum of the signal, thus the coefficients of the AR model describe the frequency changes of the signal.

$$S,k-1 \hat{\mathbf{a}}_k^- = - \sum_{i=1}^p \varphi_i S,k-i \hat{\mathbf{a}}_{k-i}^+ + \varepsilon_k \quad (3)$$

The error model Kalman filter consists in the estima-

tion of the *a posteriori* prediction errors of the acceleration and gravity from their *a priori* values and the error covariance via Kalman filtering (Luinige and Veltink, 2004). The state vector  $\mathbf{x}_{\varepsilon,k}$  is defined with the state variables  $\mathbf{a}_{\varepsilon,k}$  and  $\mathbf{g}_{\varepsilon,k}$ , corresponding to the prediction errors of acceleration and gravity, respectively (4).

$$\mathbf{x}_{\varepsilon,k} = \begin{bmatrix} \mathbf{a}_{\varepsilon,k}^T & \mathbf{g}_{\varepsilon,k}^T \end{bmatrix}^T \quad (4)$$

The bias  $\mathbf{b}_k$  is considered as noise and not as a state variable because the system is not able to distinguish between  $\mathbf{a}_k$  and  $\mathbf{b}_k$ , since both of them are unknown. Therefore, the extracted acceleration components will contain an offset due to this bias, that will be removed by high-pass filtering.

As the accelerometers do not have any external reference, their signals are referred to the sensor frame. Although the reconstructed acceleration signal norms can be directly compared between systems, both systems must have the same reference to compare the reconstructed signals to the Codamotion output for each axis. It is thus necessary to put the extracted accelerations, expressed in the local sensor frame, into the global Codamotion frame via a frame transformation. In order to do so, the constant expression of the gravity in the global frame  ${}^G\mathbf{g}$  is used. The matrix  $\mathbf{M}_k$ , called the *Rotation Matrix*, is defined as the rotation between each  ${}^{S,k}\mathbf{g}_k^+$  (gravity expressed in the sensor frame) and  ${}^G\mathbf{g}$ . Using  $\mathbf{M}_k$ , it is possible to change the reference frame of the accelerations, in order to formulate it in the global frame.

$$\begin{bmatrix} {}^G a_{x,k} \\ {}^G a_{y,k} \\ {}^G a_{z,k} \end{bmatrix} = \mathbf{M}_k \begin{bmatrix} {}^{S,k} a_{x,k}^+ \\ {}^{S,k} a_{y,k}^+ \\ {}^{S,k} a_{z,k}^+ \end{bmatrix} \quad (5)$$

Once the extracted accelerations are referenced in the global coordinate frame, they need to be multiplied by the constant of gravity  $g_C = 9.81 \text{ m/s}^2$  in order to have values in the *MKS* system of units.

## 4 EXPERIMENTAL VALIDATION

The first step was to set up a model for the prediction of the dynamic accelerations. This model has been built with the data recorded by the Codamotion for one healthy volunteer who was not part of the experimental group (pilot data). The parameters of the prediction step have been chosen experimentally. The recorded accelerations from the Codamotion were then down-sampled to match the accelerometers sampling frequency, i.e. 66,67 Hz.

Once extracted, the dynamic accelerations were high-pass filtered (cut-off frequency of 0.4 Hz) in or-

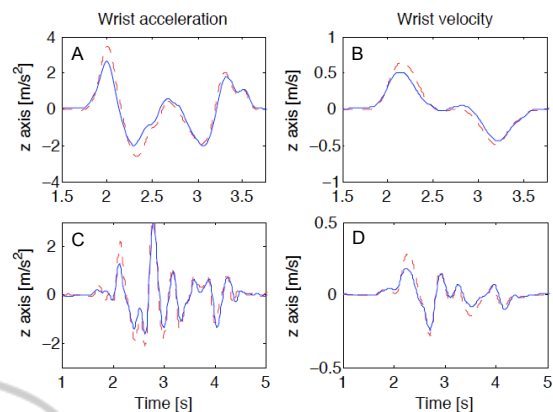


Figure 3: Accelerations and velocities for the wrist sensor. The dashed curve is the Codamotion signal while the continuous one represents the reconstructed signal from the accelerometers. Figures A and B represent the accelerations and velocities in the global  $z$  axis for a healthy volunteer, while Figures C and D represent the accelerations and velocities for a hemiparetic patient.

der to remove the remaining bias. Then, they were integrated to obtain the velocities, which have also been high-pass filtered to remove the drift. All signals were also low-pass filtered at the cut-off frequency of 5 Hz.

As the features are usually extracted on the signal norms, the reconstructed acceleration norms and the Codamotion acceleration norms have been compared, as well as axis-by-axis. The correlation coefficients ( $r$ ) and the mean square error ( $MSE$ ) between signals have been computed, for accelerations and velocities respectively, and are presented in Table 1 and 2. Even if the norms are correlated, the reconstruction is not precise enough for feature extraction. The main observation is that the best reconstruction is in the  $z$  axis, whose signals are presented in Figure 3 for a healthy volunteer and a hemiparetic patient. The  $x$  and  $y$  axes are poorly reconstructed. This is due to two different causes. The first one is the frame transformation. Indeed, only the  $z$  direction, the direction of the gravity, is known; whatever the orientation of the  $x$  and  $y$  axes,  ${}^G\mathbf{g}$  will remain the same. So, the accelerations are transformed to match the correct  $z$  direction, but not to match the directions of  $x$  and  $y$ . This problem remains for the velocities, as velocities are obtained from the integration of the acceleration signals. Secondly, according to the signals comparison, the reconstructed norm is affected by a poorly reconstruction in the  $x$  and  $y$  axes, as the  $z$  axis is very well reconstructed. The  $y$  axis gives the worst reconstruction. This direction is not really part of the movement as it is performed in the  $x-z$  plane. There are only small displacements along this axis, giving an unprecise model for the accelerations in that particular direction.

Table 1: Performances of accelerations reconstruction.

Sensor	axis	Healthy Group		Hemiparetic Group	
		$r$	$MSE$	$r$	$MSE$
Wrist	<i>norm</i>	0.608	0.790	0.675	0.374
	$x$	0.736	1.359	0.572	0.773
	$y$	-0.150	2.462	0.625	0.686
	$z$	0.934	0.284	0.899	0.239

Table 2: Performances of velocities reconstruction.

Sensor	axis	Healthy Group		Hemiparetic Group	
		$r$	$MSE$	$r$	$MSE$
Wrist	<i>norm</i>	0.437	0.092	0.635	0.063
	$x$	0.314	0.174	0.258	0.087
	$y$	-0.375	0.149	0.440	0.046
	$z$	0.949	0.008	0.875	0.010

According to these observations, the feature extraction will not be performed on the signal norms, as it is done for the Codamotion system. Indeed, the errors on the  $x$  and  $y$  axes are too large to lead to acceptable approximations of the signal norms. Instead, the feature extraction will be based on the  $z$  axis for the accelerometer-based system. Section 5 will demonstrate that the two extraction methods have the same discriminant power.

## 5 FEATURE EXTRACTION

The extracted features have already been shown discriminant between hemiparetic and healthy subjects when extracted with an optical system (Lang et al., 2006; Michaelsen et al., 2004; Chang et al., 2005; Caimmi et al., 2008). The purpose is to demonstrate that these discriminant features have the same behavior when extracted on the  $z$  axis of the reconstructed accelerations and velocities. In order to do so, random effect models (Brown and Prescott, 1999) were built using the computing environment R (Ihaka and Gentleman, 1996) and the NLME (Nonlinear and Linear Mixed Effects models) package (Pinheiro and Bates, 2006). For each feature and for each system, a random effect model was built with one fixed effect (*state*, i.e. healthy or hemiparetic) and one random effect (*subject*). The  $p$ -value associated with the fixed effect *state* determines if the output is significantly different between the two states for a given feature and a given system. As *subject* is fitted as a random effect in the models, inference is not specific to the observed subject but can be applied to the full population of subjects. For each feature, a random effect model was also built with three fixed effects

(*state*, *system*, *state*  $\times$  *system*) and two random effects (*subject*, *trial*). In this case, the  $p$ -value associated to the fixed interaction effect (*system*  $\times$  *state*) determines whether the differences between the two states are significantly different for both systems. If not, another model without the fixed interaction effect was built to determine if the extracted features were significantly different between the two systems (system effect). All data have been transformed through a log function to meet the homoscedasticity hypothesis.

TMT (Total Movement Time) has first been extracted. The correlation between sensors is statistically significant ( $r = 0.967$ ,  $p < 0.001$  for the healthy group and  $r = 0.729$ ,  $p < 0.001$  for the hemiparetic group). For both sensors, TMT is significantly shorter for the healthy group ( $p < 0.05$ ). There is neither interaction nor system effect.

The MU (Movement Unit) has then been computed on the velocities. There is no correlation between systems for the healthy group but a low significant one for the hemiparetic group ( $r = 0.479$ ,  $p < 0.05$ ). MU is significantly lower for the healthy group for both systems ( $p < 0.001$  for the Codamotion and  $p < 0.05$  for the accelerometer-based system) and there is no interaction effect. There is a significant system effect ( $p < 0.001$ ).

For the computation of the NJ (Normalized Jerk), the reach and the grasp distances have been approximated by half the arm length as those values were not available for the accelerometer-based system. For both groups, the values are correlated between systems ( $r = 0.594$ ,  $p < 0.01$  and  $r = 0.621$ ,  $p < 0.01$ ). NJ is significantly shorter for the healthy group ( $p < 0.05$  and  $p < 0.01$ ). There is no interaction effect but a significant system effect ( $p < 0.001$ ).

PWV (Peak Wrist Velocity) shows a significant correlation between the values of the two systems for the hemiparetic group ( $r = 0.661$ ,  $p < 0.001$ ) but not for the healthy group. There is no significant difference between the groups for any system but there is a system effect ( $p < 0.001$ ).

TPWV (percentage Time to Peak Wrist Velocity) does not show any significant difference or effect between groups or systems but the values are correlated between systems, for both groups ( $r = 0.695$ ,  $p < 0.001$  and  $r = 0.938$ ,  $p < 0.001$ ).

## 6 DISCUSSION

Discriminant kinematic features have been extracted from both systems in order to compare the performances of the accelerometer-based system to the Co-

Table 3: Mean features values.

Feature	Healthy		Hemiparetic	
	Accel.	Coda.	Accel.	Coda.
TMT (s)	2.134	2.094	3.613	3.624
MU (-)	3.194	2.027	6.625	4.875
NJ (-)	69.33	54.95	297.3	229.2
PWV (m/s)	0.557	0.865	0.465	0.599
TPWV (%)	33.78	30.01	30.45	27.06

damotion, used as ground truth. These kinematic features, i.e. TMT, MU, NJ, PWV and TPWV have been extracted on the  $z$  axis of the reconstructed signals for the accelerometer-based system and on the signal norms for the Codamotion. All features were significantly correlated between systems, for both groups, except for MU and PWV in the healthy group. TMT, MU and NJ have been found to be discriminant features, as expected, while PWV and TPWV have not. However, the important observation is that both systems are discriminant for TMT, MU and NJ, and not discriminant for PWV and TPWV, leading to the same discriminant and non-discriminant features. There is no interaction effect for any feature, which means that the discriminant power of the features does not depend on the system used. For features based on time, i.e. TMT and TPWV, there is no system effect, which means that their value does not depend on the system used to acquire the data. There is a system effect for MU, NJ and PWV, suggesting that the measured value depends on the system used. Indeed, those features are not extracted on the same signals, one being extracted on the  $z$  dimension while the other is on the norm. The values can thus not be similar, which leads to a system effect; however, once again, this effect has no impact on the discriminant faculty of the features.

## 7 CONCLUSIONS

Some evident limitations of visual marker-based systems are that they are expensive and not usable in the daily clinical practice. However, their precision is valuable for the extraction of kinematic features, that are essential to quantify stroke rehabilitation processes. A low-cost accelerometer-based system has been developed to address these drawbacks. A Complementary Kalman Filter has been set up in order to separate the recorded signals from the accelerometers in dynamic accelerations due to movements and gravity components. The dynamic accelerations were placed into a global frame, instead of the sensor frame, in order to draw a direct comparison with the accelerations recorded by the Codamotion system, used as ground truth. The 3-axis accelerations

and velocities have been compared between healthy and hemiparetic subjects performing reach and grasp movements, showing the best reconstruction in the  $z$  axis, while the reconstructed norms were not precise enough to be used for kinematic analyses. Feature extraction was thus performed on the reconstructed  $z$  axis for the accelerometer-based device and on the norm for the Codamotion signals. Despite of that, the accelerometer system allowed the computation of features with a discriminant power comparable to the ones derived from the Codamotion. Similar results were obtained for the sensors and markers placed on the index nail and on the thumb nail of the subjects. This accelerometer-based device is a promising alternative to expensive visual marker-based systems for rehabilitation processes, that could be used during rehabilitation sessions or at home.

A larger set of patients should be formed, as well as multiple recordings, in order to assess the evolution of the features all along the rehabilitation process. Other features could also be extracted to allow a deeper quantification of the movements. For example, the Peak Wrist Acceleration (PWA) and the percentage time to reach this value (TPWA) could be used as more sensitive features to evaluate force generation and control strategy. Indeed, the accelerometer-based system records accelerations, that are directly related to force generation. Marker-based systems use velocities for the evaluation of force generation and control strategy because this measure is more accurate as it is the first derivative of the recorded position while the acceleration is the second derivative.

## ACKNOWLEDGEMENTS

The work of JS was supported by a FRIA grant. The work of YV and the purchase of the Codamotion system was supported by the following grants: Fonds de la Recherche Scientifique Médicale (FRSM) 3.4.525.08.F 2008 & 2010; Université catholique de Louvain (UCL) Fonds Spécial de Recherche (FSR) 2008 & 2010. The work of SL was supported by UCL FSR grants 2008 & 2010.

## REFERENCES

- Brown, H. and Prescott, R. (1999). Applied mixed models in medicine, statistics in practice. *Chichester, NY: John Wiley&Sons.*
- Caimmi, M., Carda, S., Giovanzana, C., Maini, E. S., Sabatini, A. M., Smania, N., and Molteni, F. (2008). Using kinematic analysis to evaluate Constraint-Induced

- Movement Therapy in chronic stroke patients. *Neurorehabilitation Neural Repair*, 22:31–39.
- Chang, J. J., Wu, T., Wu, W. L., and Su, F. C. (2005). Kinematical measure for spastic reaching in children with cerebral palsy. *Clinical Biomechanics*, 20:381–388.
- Cirstea, M. C. and Levin, M. F. (2007). Improvement of arm movement patterns and endpoint control depends on type of feedback during practice in Stroke survivors. *Neurorehabilitation Neural Repair*, 21:398–411.
- Higgins, W. T. (1975). A comparison of complementary and Kalman filtering. *IEEE Transactions on Aerospace and Electronic Systems*, 11(3):321–325.
- Ihaka, R. and Gentleman, R. (1996). R: A language for data analysis and graphics. *Journal of computational and graphical statistics*, 5(3):299–314.
- Kavanagh, J. J. and Menz, H. B. (2008). Accelerometry : A technique for quantifying movement patterns during walking. *Gait & Posture*, 28:1–15.
- Lang, C. E., Wagner, J. M., Edwards, D. F., Sahrman, S. A., and Dromerick, A. W. (2006). Recovery of Grasp versus Reach in people with hemiparesis post-stroke. *Neurorehabilitation Neural Repair*, 20:444–454.
- Luinge, H. J. and Veltink, P. H. (2004). Inclination measurement of human movement using a 3-D accelerometer with autocalibration. *IEEE Transactions on Neural Systems and Rehabilitation Engineering*, 12(1):112–121.
- Michaelson, S. M., Jacobs, S., Roby-Brami, A., and Levin, M. F. (2004). Compensation for distal impairments of grasping in adults with hemiparesis. *Experimental Brain Research*, 157:162–173.
- Pinheiro, J. and Bates, D. (2006). Linear and nonlinear mixed effects models. *R package version*, pages 3–10.
- Trombly, C. A. (1993). Observations of improvement of reaching in five subjects with left hemiparesis. *Journal of Neurology, Neurosurgery, and Psychiatry*, 56:40–45.
- Welch, G. and Bishop, G. (2001). An introduction to the kalman filter. In Addison-Wesley, editor, *SIGGRAPH 2001 course 8. In Computer Graphics*. ACM Press.
- Wu, C., Chen, C., Tang, S. F., Lin, K., and Huang, Y. (2007). Kinematic and clinical analyses of upper-extremity movements after Constraint-Induced Movement Therapy in patients with stroke : A randomized controlled trial. *Archives of Physical Medicine and Rehabilitation*, 88:964–970.
- Wu, C., Trombly, C. A., Lin, K., and Tickle-Degnen, L. (2000). A kinematic study of contextual effects on Reaching performances in persons with and without Stroke : Influences of object availability. *Archives of Physical Medicine and Rehabilitation*, 81:95–101.
- Zhou, H. and Hu, H. (2008). Human motion tracking for rehabilitation - A survey. *Biomedical Signal Processing and Control*, 3:1–18.
- Zhou, H., Stone, T., Hu, H., and Harris, N. (2008). Use of multiple wearable inertial sensors in upper limb motion tracking. *Medical Engineering & Physics*, 30:123–133.